http://pmse.scu.edu.cn

60 ℃条件下尼龙6的熔融和重结晶行为

张 睿[1,2,3]，于博士[1,3]，杜梦雪[4]，Katalee Jariyavidyanont[4]，徐 董[1]
Christoph Schick[5]，René Androsch[4]

（1. 浙江金田高分子材料研究院有限公司，浙江 温州 325802；2. 复旦大学 高分子科学系，上海 200433；3. 安徽金田高新材料股份有限公司，安徽 安庆 231400；4. 马丁•路德大学 哈雷-维滕贝格转化导向的自然科学研究跨学科中心，德国哈雷（萨勒）D-06120；5. 罗斯托克大学 物理研究所&CALOR°协同中心，德国罗斯托克市 D-18051）

摘要：在工业生产尼龙6产品的过程中，常在玻璃化转变温度（T_g=60 ℃）进行退火，在后续加工过程中会伴随着重结晶过程的发生。文中通过快速差示扫描量热仪（FSC）表征在60 ℃退火结晶的尼龙6，观察其在升温速率10~20000 K/s范围内的重结晶行为。结果显示，其初始晶体熔点为64 ℃，仅比退火温度高4 K，此时晶体完整度低。另外，当升温速率高于1000 K/s时候，冷结晶峰在升温曲线上消失。当升温速率为20000 K/s时，仅有1个吸热峰在升温曲线被观察到，说明重结晶在该升温速率下能被抑制。

关键词：尼龙6；快速差示扫描量热仪；重结晶
中图分类号：TQ323.6 **文献标识码：**A **文章编号：**1000-7555（2025）07-0102-07

尼龙6是重要的工程塑料，在加工过程中，通常会在60 ℃预先水浴，使其达到饱和吸水状态，然后再进行进一步加工。虽然尼龙6的玻璃化转变温度在60 ℃附近，若长时间保存在此温度下，尼龙6仍然可能形成晶体。这种在玻璃化转变温度附近恒温退火形成晶体的情况已在多种聚合物中发现[1~5]。在高过冷度下结晶，通常晶体的完善程度较差[6~8]，若再次加热至高温，不完善的晶体随温度的升高会通过一个复杂的熔融-结晶过程变得逐渐完善，这种完善过程被称作重结晶过程[9,10]。

对于尼龙6熔融重结晶行为的研究，日本东丽公司走在世界前列。2015年，东丽公司的科学家Yoshimoto Furushima被派往德国罗斯托克大学，利用先进热分析设备从事相关研究[10~12]。在同步双向拉伸尼龙6薄膜生产中，流延铸片后的尼龙片，由于急冷，结晶度低，但在随后的双向拉伸过程中，温度上升会使材料本身发生熔融重结晶，而熔融重结晶会导致材料的流动特征和模量变化，进而关系到薄膜拉伸过程的破膜效应。因此，研究尼龙6的熔融重结晶过程，有助于提高生产双向拉伸尼龙薄膜的品质。除此之外，升温过程的重结晶行为本身也是经典结晶成核理论尚未完全理解的领域[13~15]。

对升温过程中聚合物的结晶和熔融行为研究中，快速差示扫描量热仪（FSC）扮演了关键作用。较传统差示扫描量热仪（DSC），FSC将热电偶和加热器集成在一个几十微米尺寸的芯片传感器上，从而可以在保持较好的信号情况下，大幅度减少测试样品所需的质量[16]。纳克数量级的样品，较DSC样品，其样品本身的比热容小，从而在液氮环境下（83 K），甚至可实现高达1 MK/s的扫描速率[17]。FSC最为广泛的应用是对聚合物的结晶成核进行研究，如模板研究所示[2,4]。同时在薄膜生产相关的基础科学领域也有大量的使用。基于FSC，Akihiko Toda和Yoshimoto Furushima等对结晶聚合物的熔融行为开

doi: 10.16865/j.cnki.1000-7555.2025.0114
收稿日期：2024-06-21
基金项目：温州市重大科技创新“揭榜挂帅”攻关项目（ZG2023044）；安徽省重点研发计划（202304a05020081）
通讯联系人：张睿，主要从事高分子物理、高分子结晶、高分子热分析和高分子材料加工等领域研究，E-mail: rui.zhang@gettel.cn

展了一系列的研究[10,14,18~23]。另外,FSC在聚合物的退火峰性质上的研究也扮演了重要作用。通常在薄膜流延工艺上,材料是一个逐步降温的过程,如用量热法再加热测试,曲线在主熔融峰温度以下往往会形成一个或多个退火峰。对于退火峰的形成,有观点认为是晶体束缚态下非晶区的松弛[24~27]。而通过FSC的表征,退火峰更支持是不完善结晶的观点[3,6,21,23,28]。

本文通过FSC对尼龙6在60 ℃结晶后的熔融重结晶行为进行了分析。重点表征了原始晶体的熔点和重结晶被抑制的升温速率,结果显示,初始晶体的熔点仅仅比退火温度高4 ℃,且需要在20000 K/s的升温速率才能抑制重结晶,该结论对进一步指导优化尼龙6的加工工艺有重要作用。

1　实验部分

1.1　主要原料

尼龙6:牌号1032,华峰集团有限公司,黏均分子量大约为2.4×10^4。使用前在80 ℃的鼓风烘箱中干燥12 h。

1.2　快速差示扫描量热仪

扫描速率10~600 K/s的实验采用商业化FSC固件由梅特勒-托尼多公司提供,商品名Flash DSC[1#][29]。与之配套的MultiSTAR USF1芯片传感器,由梅特勒-托尼多公司提供,其制造商为荷兰Xensor-Integration[30]。

扫描速率1000 K/s以上的实验采用的FSC固件由德国罗斯托克功能材料协会(Funktionale Materialien Rostock e.V.)提供,下称RFSC。该固件是一套准商业化的FSC固件,已在相关文献报道[31,32]。用于与FSC固件配套的芯片传感器是由荷兰Xensor-Integration提供的XI-395。测试环境为液氮环境(83 K),保护气体为高纯氮气。

1.3　测试过程

FSC实验采用如下扫描程序,对在60 ℃结晶的尼龙6重结晶行为进行研究。首先,尼龙6在277 ℃退火0.05 s用于去除热应力史。其次,利用设备在测试条件下的极限冷却速率将样品快速冷却至60 ℃,并在这个温度退火1000 s使样品结晶,准备工作验证,该退火形成的晶体会产生约17.4 J/g的熔融焓,参比ATHAS databank尼龙6的理论熔融焓230 J/g[33],计算结晶度约为7.6%;但是在60 ℃结晶,尼龙的晶体主要是γ相,γ相的理论熔融焓低于α相,故实际的结晶度高于7.6%。对于Flash DSC和RFSC,冷却速率分别是5000 K/s和50000 K/s。

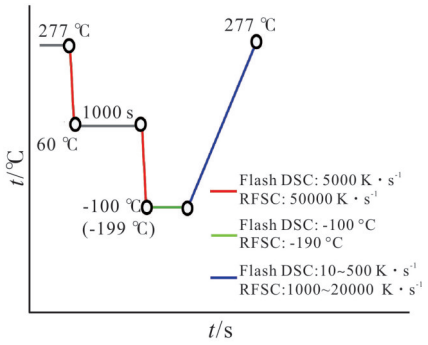


Fig. 1　FSC experiment temperature-time scanning program

2　结果与讨论

在60 ℃退火1000 s的样品,以10~2000 K/s的速率加热至熔融状态。当升温速率为10~500 K/s时,加热曲线上存在2个吸热峰和1个放热峰。吸热峰对应的是晶体熔融过程,放热峰对应的是结晶过程。根据Minakov等利用FSC研究聚合物熔融重排[34,35]可得出,60 ℃恒温退火形成的晶体在升温至一定温度发生熔融,出现第1个吸热峰。随着系统温度继续上升,此时分子链段的运动得到充分释放,同时系统温度远远低于熔点,可以提供足够的过冷度去提供结晶所需能量,故而,紧接着第1个吸热峰后出现的放热峰对应于重结晶过程。当温度继续上升,重结晶形成的晶体再次融化,形成第2个结晶峰。需要注意的是,吸热峰和放热峰的面积通常也是熔融和重结晶过程叠加的结果,并不全是单一因素行为。当升温速率达到2000 K/s时,放热峰在升温曲线上不能被观察到,高温区的吸热峰也逐渐向低温区移动,这是因为在快速升温条件下,重结晶过程被抑制。这里需要再次指出的是,尼龙6的玻璃化转变区也在60 ℃附近,玻璃化转变区附近的第1个熔融峰常被误认为是松弛峰,但是Schick等的系列研究结果证实其实质是熔融峰和松弛峰的结合[3,23,28],这也很好地符合其在图中峰宽较宽的实验结果。本文最终2个峰在20000 K/s的升温速率下合并成了1个峰,进一步支持了这个结论。

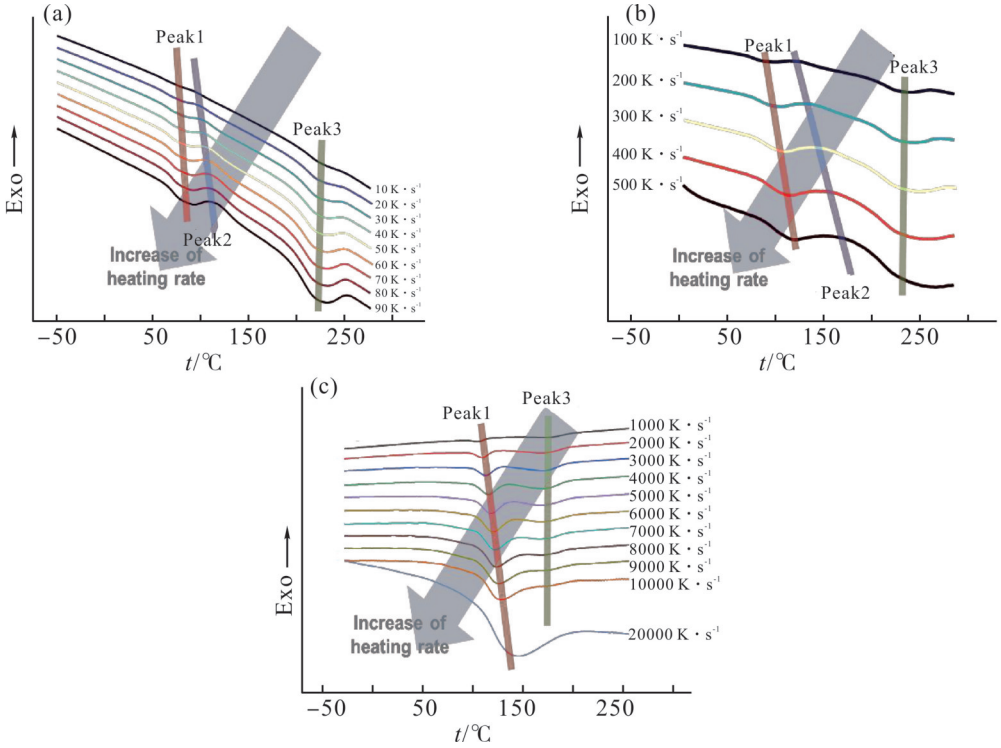


Fig. 2 FSC curves at different heating rates: (a) the FSC curve at a heating rate of 10~90 K/s; (b) the FSC curve at a heating rate of 100~500 K/s; (c) the FSC curve at a heating rate of 1000~20000 K/s

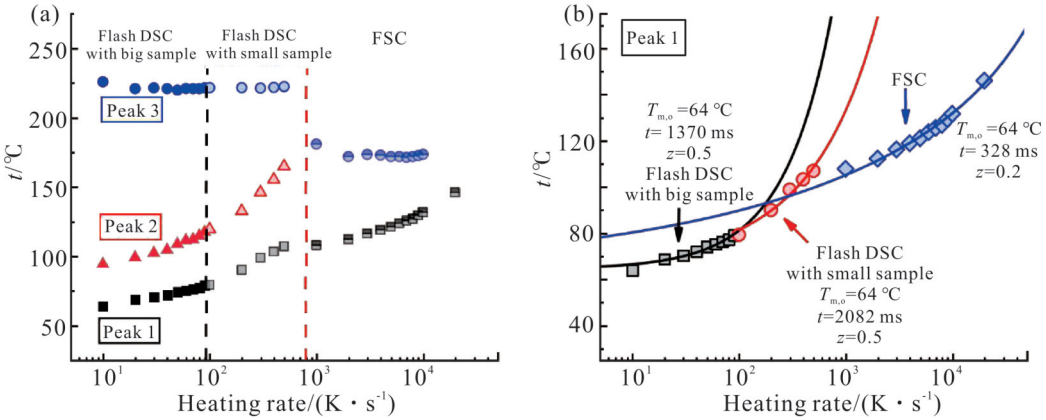


Fig. 3 (a) Relationship between the initial melting peak (Peak 1), cold crystallization peak (Peak 2), final melting peak (Peak 3), and the heating rate; (b) relationship between the initial melting peak (Peak 1) and the heating rate, and fitting it using Equation (1)

升温速率与结晶熔融峰的位置关系可用于分析重结晶动力学。考虑到不对称性，升温曲线中熔融、冷结晶峰对应温度通过使用 Asymmetric Double Sigmoidal Function 拟合来确定。Fig.3(a)展示了熔融、冷结晶峰位置于对应升温速率的关系，其中 Peak 1，Peak 2 和 Peak 3 分别对应 Fig.2 中的低温熔融峰、冷结晶峰、高温熔融峰。Peak 1 是低温熔融峰，其峰位置很大程度上依赖于未发生重结晶晶体的尺寸和热延迟[3,9,10,14,23,36]。尽管本文由2种不同的芯片传感器和3个不同大小的样品完成，Peak 1 的数据仍然保持了较好的一致性，未出现明显断档，细节将随后讨论。Peak 2 是升温过程中的冷结晶峰，其实质是晶体重结晶的重排过程。随着升温速率由 10 K/s 提高至 500 K/s，Peak 2 向高温区移动，由 94 ℃上升至 165 ℃，说明重结晶随升温速率的上升被逐渐压制。当升温速率超过 1000 K/s (对应 Fig.2(c))，

Peak 2将不能在升温曲线中观察到。需要指出的是此时升温曲线仍然存在Peak 1和Peak 3,说明重结晶仍然没有被完成压制,只是Peak 1,Peak 2和Peak 3的叠加效应使得Peak 2被掩盖,不能被观测到。该现象在Toda和Furushima的系列研究中有较详细的论证,不在此处重复展开。由Fig.2(c)所知,当升温速率高达20000 K/s时候,升温曲线中只有1个吸热峰,在146 ℃,说明此时重结晶被完全压制。Peak 3是最终的晶体熔融峰。Flash DSC和FSC的Peak 3出现了不一致的情况。第1种可能是重结晶逐渐被压制,Peak 2逐渐移向高温区,渐渐靠近Peak 3,最终出现重叠效应[10]。出现该情况的先决条件是尼龙6是一种结晶速率快的聚合物。虽然尼龙6是短烯烃链的尼龙,但是分子相互作用强[37,38],其熔体构象熵更低,更容易通过构象熵驱动结晶行为的发生[2,39,40],而与以上特殊现象吻合。

Fig.3(b)是截取Peak 1与升温速率的关系图,其将根据Toda等的方法,并考虑热延迟情况,对3次测试结果分别进行拟合[3,9,19,41]

$$T_m = T_{m,0} + \tau * \beta + C * \beta^z \quad (1)$$

式中:T_m——测量的表观熔点,对应Peak 1;$T_{m,0}$——零熵熔融温度,是熔点外推到无升温速率依赖状态下的值;β——升温速率;C——常数项;z——Toda提出的Superheating指数项,用于修正高速条件熔点与升温速率在对数条件下偏离线性的情况,其值通常为(0.1~0.5)[9]。拟合结果显示,$T_{m,0}$=64 ℃(退火温度+4 K),说明在60 ℃的退火结晶过程,晶粒生长是有限的,不完美程度高,也印证后续重结晶的发生。Flash DSC测试的热延迟在10^3 μs数量级,而FSC测试的热延迟在10^2 μs数量级,主要是因为FSC测试所用的芯片传感器更小,样品更小,厚度因此也被大大减薄[16]。

Fig.3(b)中,Peak 1, Peak 2和Peak 3的z值分别是0.5,0.5和0.2,均在0~0.5的范围内,符合用式(1)分析的要求。但是,z与样品的尺寸应该是不存在依赖性[10,16,42,43]。对于z值出现异常,造成的原因可能是Peak 1的面积同时包含松弛焓和熔融焓。60 ℃刚好是尼龙6的玻璃化转变温度附近,长时间退火会产生少量松弛焓[2,4,5]。松弛焓最大值可以由玻璃化转变温度对应的比热容台阶乘以玻璃化转变温度与退火温度之差估计($\Delta c_p \times (T_g - T_a)$),由此可见其数值很小。同时,当松弛过程接近尾声的时候,结晶发生,晶体熔化的时候产生熔融焓[44]。尼龙6的半结晶时间大约为5 s[45],故而在退火1000 s后,晶体在该退火温度下,已经接近尾声,其峰受到松弛焓的影响,但是主要还是取决于熔融焓。据此分析,可以理解虽然z值存在差异,但是$T_{m,0}$的数值均为64 ℃。

3　结论

通过表征60 ℃预结晶的尼龙6,在10~20000 K/s升温速率下的重结晶行为,得到以下三点主要结论。

(1)60 ℃预结晶的尼龙6,其初始晶体为64 ℃,仅比退火温度高4 K,表明其晶体完善程度不高。

(2)当升温速率达到1000 K/s,冷结晶峰在升温曲线中消失。在此处冷结晶峰是由于重结晶引起的。

(3)当升温速率高达20000 K/s,升温曲线上仅能观察到1个吸热峰,说明重结晶在该温度被抑制。

以上结论诠释了尼龙6在加工工程容易出现重结晶的现象,同时也指出,这类现象是很难通过改善工艺来避免的,需通过调节其熔体稳定性来改善[46,47]。

参考文献:

[1] Zhang R, Zhuravlev E, Schmelzer J W P, *et al.* Steady- state crystal nucleation rate of polyamide 66 by combining atomic force microscopy and fast- scanning chip calorimetry[J]. Macromolecules, 2020, 53: 5560-5571.

[2] Zhang R, Jariyavidyanont K, Du M, *et al.* Nucleation and crystallization kinetics of polyamide 12 investigated by fast scanning calorimetry[J]. Journal of Polymer Science, 2021, 60: 842-855.

[3] Zhang R, Jariyavidyanont K, Zhuravlev E, *et al.* Zero- entropy-production melting temperature of crystals of poly(butylene succinate) formed at high supercooling of the melt[J]. Macromolecules, 2022, 55: 965-970.

[4] Zhuravlev E, Schmelzer J W P, Wunderlich B, *et al*. Kinetics of nucleation and crystallization in poly(ε- caprolactone) (PCL) [J]. Polymer, 2011, 52: 1983-1997.

[5] Jariyavidyanont K, Zhuravlev E, Schick C, *et al*. Kinetics of homogeneous crystal nucleation of polyamide 11 near the glass transition temperature[J]. Polymer Crystallization, 2021, 4: e10149.

[6] Jariyavidyanont K, Zhang R, Yu Q, *et al.* Formation of imperfect crystals in poly(ε- caprolactone) at high melt- supercooling[J]. Materials Letters, 2022, 324: 132704.

[7] Jariyavidyanont K, Schick C, Androsch R. The bulk enthalpy of melting of α'-crystals of poly (L-lactic acid) determined by fast scanning chip calorimetry[J]. Thermochimica Acta, 2022, 717: 179349.

[8] Jariyavidyanont K, Du M, Yu Q, *et al*. Bulk enthalpy of melting of poly (l-lactic acid) (PLLA) determined by fast scanning chip calorimetry[J]. Macromolecular Rapid Communications, 2022, 43: 2200148.

[9] Toda A, Androsch R, Schick C. Insights into polymer crystallization and melting from fast scanning chip calorimetry [J]. Polymer, 2016, 91: 239-263.

[10] Furushima Y, Schick C, Toda A. Crystallization, recrystallization, and melting of polymer crystals on heating and cooling examined with fast scanning calorimetry[J]. Polymer Crystallization, 2018, 1: e10005.

[11] Furushima Y, Nakada M, Ishikiriyama K, *et al.* Two crystal populations with different melting/reorganization kinetics of isothermally crystallized polyamide 6[J]. Journal of Polymer Science Part B: Polymer Physics, 2016, 54: 2126-2138.

[12] Melnikov A P, Rosenthal M, Rodygin A I, *et al*. Re-exploring the double-melting behavior of semirigid-chain polymers with an in-situ combination of synchrotron nanofocus X-ray scattering and nanocalorimetry [J]. European Polymer Journal, 2016, 84: 598-606.

[13] Andrianov R A, Androsch R, Zhang R, *et al*. Growth and dissolution of crystal nuclei in poly(L- lactic acid) (PLLA) in Tammann's development method[J]. Polymer, 2020, 196: 122453.

[14] Furushima Y, Nakada M, Murakami M, *et al*. Method for calculation of the lamellar thickness distribution of not-reorganized linear polyethylene using fast scanning calorimetry in heating[J]. Macromolecules, 2015, 48: 8831-8837.

[15] Mukhametzyanov T, Schmelzer J W P, Yarko E, *et al.* Crystal nucleation and growth in cross- linked poly(ε- caprolactone) (PCL) [J]. Polymers, 2021, 13: 3617.

[16] Schick C, Mathot V. Fast scanning calorimetry[M]. Springer International Publishing AG Switzerland, 2016.

[17] Minakov A A, Schick C. Ultrafast thermal processing and nanocalorimetry at heating and cooling rates up to 1 MK/s[J]. Review of Scientific Instruments, 2007, 78: 073902.

[18] Furushima Y, Toda A, Rousseaux V, *et al.* Quantitative understanding of two distinct melting kinetics of an isothermally crystallized poly(ether ether ketone) [J]. Polymer, 2016, 99: 97-104.

[19] Toda A, Taguchi K, Nozaki K, *et al.* Superheated melting kinetics of metastable chain- folded polymer crystals[J]. Crystal Growth & Design, 2018, 18: 3637-3643.

[20] Toda A, Taguchi K, Nozaki K. Fast limiting behavior of the melting kinetics of polyethylene crystals examined by fast- scan calorimetry[J]. Thermochimica Acta, 2019, 677: 211-216.

[21] Androsch R, Toda A, Furushima Y, *et al*. Insertion-crystallization-induced low- temperature annealing peaks in melt- crystallized poly(L-lactic acid) [J]. Macromolecular Chemistry and Physics, 2021, 222: 2100177.

[22] Toda A, Furushima Y, Androsch R, *et al*. On the crystal stabilization during two- step isothermal crystallization of poly (butylene terephthalate) examined by fast scanning calorimetry [J]. Polymer, 2021, 230: 124057.

[23] Schick C, Toda A, Androsch R. The narrow thickness distribution of lamellae of poly(butylene succinate) formed at low melt supercooling[J]. Macromolecules, 2021, 54: 3366-3376.

[24] Xie Z N, Ye H M, Chen T, *et al.* Melting and annealing peak temperatures of poly(butylene succinate) on the same Hoffman-weeks plot parallel to $t_m=t_c$ line[J]. Chinese Journal of Polymer Science, 2020, 39: 745-755.

[25] Wei Z, Song P, Zhou C, *et al*. Insight into the annealing peak and microstructural changes of poly(L- lactic acid) by annealing at elevated temperatures[J]. Polymer, 2013, 54: 3377-3384.

[26] Bonnet M, Rogausch K D, Petermann J. The endothermic "annealing peak" of poly (phenylene sulphide) and poly (ethylene terephthalate) [J]. Colloid and Polymer Science, 1999, 277: 513-518.

[27] Zhang R, Jariyavidyanont K, Zhuravlev E, *et al*. Physical aging and glass transition dynamics of semicrystalline poly(lactic acid)

for 3d- printing applications investigated by fast scanning calorimetry[J]. Macromolecules, 2024, 57: 32-41.

[28] Schick C, Androsch R. The origin of annealing peaks in semicrystalline polymers: enthalpy recovery or melting?[J]. Macromolecules, 2020, 53: 8751-8756.

[29] Mathot V, Pyda M, Pijpers T, *et al*. The flash DSC 1, a power compensation twin- type, chip- based fast scanning calorimeter (FSC): first findings on polymers[J]. Thermochimica Acta, 2011, 522: 36-45.

[30] Van H S, Iervolino E, Van H F, *et al.* Design, performance and analysis of thermal lag of the UFS1 twin- calorimeter chip for fast scanning calorimetry using the Mettler- Toledo flash DSC 1 [J]. Thermochimica Acta, 2011, 522: 46-52.

[31] Zhuravlev E, Schick C. Fast scanning power compensated differential scanning nano- calorimeter: 1. the device[J]. Thermochimica Acta, 2010, 505: 1-13.

[32] Zhuravlev E, Schick C. Fast scanning power compensated differential scanning nano- calorimeter: 2. heat capacity analysis [J]. Thermochimica Acta, 2010, 505: 14-21.

[33] Nylon 6 (nylon6) heat capacity, enthalpy, entropy, Gibbs energy: datasheet from "the advanced thermal analysis system (Athas) databank- polymer thermodynamics" release 2014 in Springer materials. https://materials.Springer.Com/olymerthermodynamics/docs/athas_0024[EB/OL]. Springer- Verlag Berlin Heidelberg & Marek Pyda.

[34] Minakov A A, Mordvintsev D A, Schick C. Melting and reorganization of poly(ethylene terephthalate) on fast heating (1000 K/s) [J]. Polymer, 2004, 45: 3755-3763.

[35] Minakov A A, Mordvintsev D A, Tol R, *et al*. Melting and reorganization of the crystalline fraction and relaxation of the rigid amorphous fraction of isotactic polystyrene on fast heating (30,000 K/min) [J]. Thermochimica Acta, 2006, 442: 25-30.

[36] Androsch R, Zhuravlev E, Schick C. Solid- state reorganization, melting and melt- recrystallization of conformationally disordered crystals (α′- phase) of poly (L- lactic acid) [J]. Polymer, 2014, 55: 4932-4941.

[37] Li X, He Y, Dong X, *et al*. Effects of hydrogen- bonding density on polyamide crystallization kinetics[J]. Polymer, 2020, 189: 122165.

[38] Wang T, Li X, Luo R, *et al*. Effects of amide comonomers on polyamide 6 crystallization kinetics[J]. Thermochimica Acta, 2020, 690: 178667.

[39] Carfagna C, Busico V, Salerno V, *et al*. Melting behaviour of a series of monoamides[J]. Thermochimica Acta, 1980, 37: 31-36.

[40] Carfagna C, Vacatello M, Corradini P. Conformational freedom of polyamide chains above the melting point[J]. Journal of Polymer Science: Polymer Chemistry Edition, 1977, 15: 1-4.

[41] Wunderlich B. Macromolecular physics, volume 1: crystal structure, morphology, defects[M]. Netherlands: Elsevier, 1973.

[42] Minakov A A, Schick C. Nanometer scale thermal response of polymers to fast thermal perturbations[J]. The Journal of Chemical Physics, 2018, 149: 074503.

[43] Minakov A, Van H A, Wien W, *et al*. Advanced nonadiabatic ultrafast nanocalorimetry and superheating phenomenon in linear polymers[J]. Thermochimica Acta, 2007, 461: 96-106.

[44] Androsch R, Schick C. Interplay between the relaxation of the glass of random L/D- lactide copolymers and homogeneous crystal nucleation: evidence for segregation of chain defects[J]. The Journal of Physical Chemistry B, 2016, 120: 4522-4528.

[45] Zhang X, Buzinkai J, Quinn E, *et al.* Key insights into the differences between bimodal crystallization kinetics of polyamide 66 and polyamide 6[J]. Macromolecules, 2022, 55: 9220-9231.

[46] Lim L T, Auras R, Rubino M. Processing technologies for poly (lactic acid) [J]. Progress in Polymer Science, 2008, 33: 820-852.

[47] Xu G, Ding J, Yang Y. Monte Carlo simulation of self- avoiding lattice chains under slit flow[J]. Rheologica Acta, 1999, 38: 562-568.

Melting and Recrystallization of Nylon 6 at 60 ℃

Rui Zhang[1,2,3], Boshi Yu[1,3], Mengxue Du[4], Katalee Jariyavidyanont[4], Dong Xu[1], Christoph Schick[5], René Androsch[4]
(*1. Zhejiang Gettel Polymer Materials Research Institute Co., Ltd., Wenzhou 325802, China; 2. Department of Macromolecular Science, Fudan University, Shanghai 200433, China; 3. Anhui Gettel Advanced Materials Co., Ltd., Anqing 231400, China; 4. Interdisciplinary Center for Transformation-Oriented Natural Science Research, Martin Luther University Halle-Wittenberg, Halle (Saale), D-06120, Germany; 5. Institute of Physics, University of Rostock, Rostock, D-18051, Germany*)

ABSTRACT: In the industrial production of nylon 6 products, there is often an annealing process at the glass transition temperature (T_g=60 °C), and the accompanying crystallization often leads to recrystallization in the subsequent processing. In this study, a fast scanning calorimeter (FSC) was used to characterize the recrystallization behavior of nylon 6 that was crystallized at 60 °C. The results show that the initial melting point of the crystals is 64 °C, which is only 4 K higher than the annealing temperature, and the degree of crystal perfection is low. In addition, when the heating rate is higher than 1000 K/s, the cold crystallization peak disappears on the heating curve. When the heating rate is 20000 K/s, only one endothermic peak is observed in the heating curve, indicating that recrystallization is inhibited at this heating rate.

Keywords: nylon 6; fast scanning calorimeter; recrystallization